

 Open access • Posted Content • DOI:10.1101/2021.01.28.428693

Resequencing 250 soybean accessions: new insights into genes associated with agronomic traits and genetic networks — Source link

Yang Chunming, Jun Yan, Jiang Shuqin, Li Xia ...+3 more authors

Institutions: China Agricultural University, Harbin Normal University

Published on: 29 Jan 2021 - bioRxiv (Cold Spring Harbor Laboratory)

Topics: Genetic diversity, Molecular breeding and Candidate gene

Related papers:

- [Resequencing 250 Soybean Accessions: New Insights into Genes Associated with Agronomic Traits and Genetic Networks.](#)
- [The analysis of functional genes in maize molecular breeding](#)
- [Landscape of genomic diversity and trait discovery in soybean.](#)
- [Dissection of soybean populations according to selection signatures based on whole-genome sequences](#)
- [Genome-wide Scan for Seed Composition Provides Insights into Soybean Quality Improvement and the Impacts of Domestication and Breeding](#)

Share this paper:    

View more about this paper here: <https://typeset.io/papers/resequencing-250-soybean-accessions-new-insights-into-genes-3wt3vfm17i>

1 **Resequencing 250 soybean accessions: new insights into genes**
2 **associated with agronomic traits and genetic networks**

3

4 Chunming Yang^{1#}, Jun Yan^{2#}, Shuqin Jiang², Xia Li³, Haowei Min^{4*}, Xiangfeng
5 Wang^{2*}, Dongyun Hao^{1*}

6

7 ¹*Key Laboratory for Agricultural Biotechnology of Jilin Provincial, Institute of*
8 *Agricultural Biotechnology, Jilin Academy of Agricultural Sciences (JAAS), Jilin*
9 *130033, China*

10 ²*Department of Crop Genomics and Bioinformatics, College of Agronomy and*
11 *Biotechnology, China Agricultural University, Beijing 100094, China*

12 ³*Key Laboratory of Molecular Cytogenetics and Genetic Breeding of Heilongjiang*
13 *Province, College of Life Science and Technology, Harbin Normal University, Harbin*
14 *150025, Heilongjiang, China*

15 ⁴*BioTrust Technology. Inc., Beijing 100094, China*

16

17 # Equal contribution

18 * Corresponding authors

19

20 **E-mail:**

21 dyhao@cjaas.com (Hao D);

22 xwang@cau.edu.cn (Wang X);

23 biotrust_st@163.com (Min H);

24

25

26

27

28 **Running title:** Chunming Yang *et al.* / Soybean resequence

29

30

31

32 **Abstract**

33 Limited knowledge on genomic diversity and the functional genes associated with
34 soybean variety traits has resulted in slow breeding progress. We sequenced the
35 genome of 250 soybean landraces and cultivars from China, America and Europe, and
36 investigated their population structure, genetic diversity and architecture and selective
37 sweep regions of accessions. We identified five novel agronomically important genes
38 and studied the effects of functional mutations in respective genes. We found
39 candidate genes *GSTT1*, *GL3* and *GSTL3* associated with isoflavone content, *CKX3*
40 associated with yield traits, and *CYP85A2* associated with both architecture and yield
41 traits. Our phenotype-gene network analysis revealed that hub nodes play a role in
42 complex phenotypic associations. In this work, we describe novel agronomic trait
43 associated genes and a complex genetic network, providing a valuable resource for
44 future soybean molecular breeding.

45

46 **Introduction**

47 Soybean *Glycine max* [L.] Merr. is one of the most important crops worldwide of
48 vegetable oil and proteins source for human and livestock feed etc. Soybean
49 originated in China and its wild species (*G. soja* Sieb. & Zucc.) were domesticated in
50 approximately 3,000 B.C. before introduced to Korea and Japan about 3,000 years
51 later. It was brought to Europe and North America in the 18th century, and extensively
52 cultivated on a global scale since the 19th century[1].

53 With the rapid development of modern molecular biology and the
54 high-throughput sequencing technologies, whole-genome resequencing and genome
55 wide association studies (GWAS) have become common methods used to study
56 population genetic diversity and locating phenotypic related quantitative trait loci
57 (QTL) or genes. This has improved our knowledge extensively in crop genomes and

58 selective breeding. In recent years, for example, there are increasing number of
59 reports on the domestication and improvement of soybean at the genome-wide level.
60 This includes genes and genetic networks related to soybean agronomic traits and
61 functions[2-4]. However, due to the diversity of soybean varieties and their complex
62 genetic background, our knowledge of the soybean genome and functional genes is
63 still limited in comparison to rice and maize. A greater number of soybean varieties
64 need further exploration at the genomic level, particularly in relation to molecular
65 traits associated with edible quality, soybean “ideotype” and the underlying genetic
66 network of high-yielding varieties.

67 In this study, we collected 250 soybean varieties from the core Northeast China
68 soybean germplasm pool, which consisted of 134 accessions of landrace and cultivar
69 from Northeast and Northwest China, as well as 116 accessions from European and
70 North American cultivars. The genomes of the most accessions are not sequenced
71 previously. We performed the high-depth whole-genome resequencing and
72 comprehensive analyses of this 250 soybean population. The generated dataset
73 revealed valuable new information on soybean genome structure, novel genes
74 associated with important agronomic traits and the genetic networks. These genetic
75 resources provide unique references into molecular breeding and evolution study in
76 soybean.

77

78 **Results**

79 **Genome resequencing and variation calling**

80 High-depth whole genome resequencing was performed on 250 soybean accessions,
81 including 51 landraces and 83 cultivars originating from provinces in Northeast China
82 (i.e. Heilongjiang, Jilin, Liaoning and Northeast Inner Mongolia) and Northwest
83 China (i.e. Xinjiang, Ningxia and Gansu), as well as 116 cultivars originating from
84 Europe and North America (**Figure 1a, Supplementary Table 3**). In total, we
85 obtained approximately 10G of pair-end reads and 3T bases. The maximum
86 sequencing depth of a single accession was 22.5x, with the average depth at 11x. After

87 filtering out the raw sequencing data (see methods), the remaining high-quality
88 cleaned data were compared with the soybean reference genome *G. max* v2.0[5]. The
89 effective mapping rates ranged from 74.8% to 87.6%, while the genome coverage
90 ranged from 94.8% to 97.0% (**Supplementary Table 1**). The high mapping rates and
91 coverage guarantee that the sequenced data is reliable and of high quality.

92 Through standard variation detection, genotype filtering and imputation steps
93 (see methods), we detected in total 6,333,721 single nucleotide polymorphisms (SNPs)
94 and 2,565,797 insertion & deletions (Indels). This includes 244,360 SNPs and 62,714
95 Indels located in the exon regions. The ratio of non-synonymous SNP to synonymous
96 SNP substitution was 1.37. There are 4,311,814 SNPs with a minor allele frequency
97 (MAF) larger than 0.05 (**Supplementary Table 2 & Supplementary Figure 1**). In
98 summary, we achieved over 6M high-density and high-quality genotype data from
99 250 soybean accessions with a density of one SNP per 15 bases.

100

101 **Population structure of soybean landraces and cultivars**

102 Using the 6M SNP genotype dataset, we constructed a phylogenetic tree using the
103 neighbour joining (NJ) method. This resulted in the classification of the 250 soybean
104 accessions into four groups (**Figure 1b**). Among them, *Group 1* included 65 Chinese
105 varieties, four European and six American cultivars, whereas *Group 2* contained 56
106 Chinese varieties, one European and 13 American varieties. In *Group 3*, there were 21
107 European, two Chinese and six American cultivars, while 65 North American
108 cultivars and 11 Chinese varieties were clustered within *Group 4* (**Figure 1c**).
109 Principal Component Analysis (PCA) results were consistent with the phylogenetic
110 tree results. Three groups, *Group 1*, *3*, and *4* radiated away from *Group 2* within the
111 rectangular coordinate system projected using eigenvector 1 and eigenvector 2 data on
112 X and Y axes, respectively. Concurrently, the distribution of varieties in the four
113 groups had continuity, indicating varieties located in different groups also have
114 genetic similarities (**Figure 1e**). A Bayesian clustering algorithm based on a mixed
115 model was used to estimate the proportion of ancestors in each accession. That is,
116 when $K = 2$, the main ancestor component (yellow) of *Group 4* was split, indicating

117 that *Group 4* has the highest level of selection. When $K = 3$, the main ancestor
118 component (blue) of *Group 3* was split, indicating that *Group 3* has the second level
119 of selection. However, when $K = 4$ and $K = 5$, *Group 1* and *Group 2* exhibit complex
120 differentiated mixed ancestor components, indicating a higher genetic diversity and
121 lower selection level in *Groups 1* and *2* (**Supplementary Table 3, Figure 1d**).

122 These results indicate that group classification of the 250 soybean accessions is
123 closely related to their geographical distribution. That is, varieties with similar
124 geographical distribution have similar genetic backgrounds. Generally speaking, the
125 group classification was also related to the level of domestication. Landraces have a
126 lower level of domestication, while cultivars have higher levels of domestication.
127 Varieties with similar domestication levels tend to have a higher similarity in genetic
128 backgrounds. However, there are still differences in geographical distribution and
129 domestication level among breeds with similar genetic backgrounds, indicating that
130 gene exchange may have occurred between accessions of different groups. This
131 observation reflected the complexity of soybean domestication history.

132

133 **Genetic diversity and selective sweep analysis**

134 Linkage disequilibrium (LD) analysis showed that the overall LD decay distance was
135 more than 100 kb, and the LD decay distance of the landraces was smaller than that of
136 the cultivars (**Figure 2A**). Further LD decay analysis of the four groups showed that
137 the LD decay distance of *Group 1* was the smallest, followed by *Groups 2* and *3*,
138 while *Group 4* had the largest LD decay distance (**Figure 2B**). In addition, the LD
139 levels varied for different chromosomes or different regions across one chromosome.
140 Identical by state (IBS) analysis can reflect the degree of relatedness among
141 individuals by calculating the consistency of all genetic markers. The IBS values of
142 all comparisons in each group were calculated, and it was found that the average IBS
143 values of landraces were less than that of cultivars (**Figure 2C**). The IBS values of
144 *Groups 1-4* followed the same trends as that of LD decay distance. In particular, the
145 IBS values of *Group 1* were the lowest and the IBS values of *Group 4* were the
146 highest of all groups (**Figure 2D**). $\theta\pi$ values can reflect the genetic diversity within a

147 population by calculating the number of different sites between any two sequences or
148 individuals within a population. F_{st} is a calculation used to measure the
149 differentiation and genetic distance between two populations. $\theta\pi$ values were
150 calculated for landraces, cultivars, all accessions, and *Groups 1-4*. F_{st} values were
151 calculated between landraces and cultivars, and between each comparison of the four
152 Groups. Results show that a population with a higher level of LD decay distance or
153 higher IBS values correlate with a smaller $\theta\pi$ (**Figure 2E, F**). This pattern is opposite
154 to that of the LD decay and IBS values. The lowest F_{st} value was for *Group 1* versus
155 *Group 2*, while the highest value was for *Group 3* versus *Group 4*. We also observed
156 that the F_{st} value of *Group 2* versus *Group 3* was higher than that of *Group 1* versus
157 *Group 3* (**Figure 2G**). The F_{st} value of *Group 2* versus *Group 4* was smaller than that
158 of *Group 1* versus *Group 4*. In addition, the results of allele frequency distribution
159 (AFD) analysis, as an alternative population similarity measurement, were consistent
160 with the F_{st} results (**Supplementary Figure 2**). The population diversity analysis
161 results, when combined with population structure and geographical distribution
162 information, infer that the European and American soybean varieties may have
163 originated from different Chinese ancestors before undergoing independent selection.
164 Results indicate that European cultivars and the Chinese landrace group (*Group 1*) in
165 our study have a more recent common ancestor, while North American cultivars and
166 the Chinese cultivar group (*Group 2*) have a more recent common ancestor.

167 *Tajima' D* (based on a neutral test), $\theta\pi$ (based on genetic diversity within a
168 population), and F_{st} (based on genetic diversity between two populations), have
169 provided us with highly effective tools that screen selective sweep signals across a
170 genome[6]. We combined methods in pairs for mining potential selective sweep
171 regions in the soybean genome that may have underwent artificial selection. One pair
172 was *Tajima' D* combined with $\theta\pi$ for the whole population. Another pair was F_{st}
173 combined with $\theta\pi$ ratios between two subpopulations, landrace and cultivar. We used
174 a sliding window method to calculate the values of *Tajima' D*, $\theta\pi$, and F_{st} in each
175 window across the whole genome, and selected the top 5% most significant windows
176 as potential selective sweep regions (**Supplementary Figure 3A, B**). A total of 148

177 and 222 potential selective sweep regions were screened by the two methods, and they
178 covered 36.09 Mb and 88.15 Mb genome regions, respectively (**Supplementary**
179 **Table 4**). These potential selective sweep regions covered 9,128 genes, accounting for
180 approximately one sixth of all soybean genes. A total of 1,876 genes were screened by
181 both methods (**Supplementary Figure 3C**). A runs of homozygosity (ROH) region is
182 a continuous homozygous chromosome region in a genome, which may relate to
183 domestication or artificial selection[7]. Through ROH analysis, 71 ROH regions
184 larger than 300 kb were obtained from all 250 accessions, with a total length of 27.84
185 Mb. The longest ROH regions up to 911 kb were located at the beginning of
186 chromosome 10 (**Supplementary Table 5**). There were 3,397 genes located in these
187 ROH regions, 924 of which were also located in the potential selected sweep region
188 (**Supplementary Figure 3D**).

189

190 **Phenotype-related loci and genes identified using GWAS analysis**

191 We measured 50 agronomic traits in 250 soybean accessions from three geographic
192 locations for three years, and then integrated them using best linear unbiased
193 prediction (BLUP). The 50 traits included traits related to architecture (15), colour (5),
194 isoflavone (1), oil (4), protein (18) and yield (7) and were classified into six categories
195 (**Supplementary Table 6**). We calculated Pearson correlation coefficients for traits so
196 as to compare within and between categories, and found that traits in the same
197 categories were more strongly correlated than traits in different categories. For
198 example, there were strong positive or negative correlations between almost all
199 protein-related traits, oil-related traits and yield-related traits. Linoleic acid content
200 was positively correlated with linolenic acid content, but negatively correlated with
201 oleic acid content. Stem intension was negatively correlated with lodging
202 (**Supplementary Figure 4**). Some traits were evenly distributed, while others were
203 ranked (**Supplementary Figure 5-54**).

204 Using 4,311,814 SNPs with a MAF > 0.05 as an input, we performed GWAS
205 analysis using the mixed linear model (MLM) method for 50 agronomic traits. For
206 each trait, we used a clump based method[8] and defined a significant associated loci

207 (SAL) at a chromosome region with a substantial amount of SNPs associated with the
208 trait. A total of 203 SALs were detected in 43 traits (**Supplementary Figure 5-54,**
209 **Supplementary Table 7**). Since each SAL may contain dozens of genes, we used a
210 functional mutation based haplotype test method for further mining of the most
211 reliable candidate trait associated genes[9]. In particular, we considered only the
212 non-synonymous SNPs, frameshift Indels, mutations within a gene that happened on a
213 start or stop codon, splice site or transcription start sites as effective functional
214 mutations. We used these mutations to classify a gene into different haplotypes, and
215 subsequently tested the phenotypic differences of the accessions belonging to each
216 haplotype. A gene with significant phenotypic differences was defined as significant
217 associated gene (SAG), and 3,165 SAGs were screened in 43 traits. These SAGs
218 include some QTL or genes that have been previously identified, such as: the flower
219 colour related *chr13:16551728-19506795*; pubescence colour related
220 *chr6:16930159-19168772*; seed coat lustre related *chr15:8910798-10281804*;
221 palmitic acid content related *chr5:879095-1682551*[4]; isoflavone content related
222 *chr5:38880530-39142565*[10]; plant height related *Dt1*[4]; and oil content related
223 *FAD2* and *SAT1*[11], among others. They also contain genes that we have identified
224 for the first time in soybean, such as: the isoflavone content related *GL3* and *GSTL3*;
225 the yield traits related *CKX3*; and the architecture and yield traits related *CYP85A2*.

226

227 **Novel genes related to isoflavone content**

228 Isoflavone content is an important quality-related trait in soybean, but its molecular
229 mechanism is still unclear. Here we identified four SALs related to isoflavone content,
230 namely *chr3:38590023-38728718*, *chr5:3888053-39142565*,
231 *chr13:18342836-18541809*, and *chr5:24726091-24852447*. Only one SAL
232 *chr5:24726091-24852447* overlaps with a previously reported QTL that contains a
233 *GST* (Glutathione S-transferase) gene *GSTT1*[10]. All other SALs are newly identified.
234 There are 48 genes located within these SALs (**Supplementary Table 8**), and three
235 genes (*GSTT1*, *GL3* and *GSTL3*) may be related to isoflavone content (**Figure 3A, B**).
236 There are two functional mutation sites at *c5s38936266* and *c5s38940717*, forming

237 two haplotypes for *GSTT1a* and *GSTT1b*, respectively. For each *GSTT1* gene, soybean
238 accessions with a different haplotype have significantly different isoflavone contents.
239 Since *GSTT1a* and *GSTT1b* are approximately only 1 kb apart from each other in the
240 same genome region, we considered the two genes to be one in further analysis. Three
241 haplotypes were formed by two functional mutation sites when the two *GSTT1* genes
242 were analysed as one. *Haplotype 1* versus *Haplotype 2*, as well as *Haplotype 2* versus
243 *Haplotype 3* showed significant differences in isoflavone content, while *Haplotype 1*
244 versus *Haplotype 3* showed no significant differences (analysed using Tukey's test).
245 This suggests that *GSTT1a* is associated with isoflavone content due to its linkage
246 with *GSTT1b*. However, *c5s38936266* did not contribute to the isoflavone content
247 difference. Thus, only *c5s38940717* on *GSTT1b* was associated with isoflavone
248 content (**Figure 3C**).

249 We found that two functional mutations, *c5s39035509* and *c5s39036346*
250 producing two haplotypes in *GL3*, were associated with different isoflavone contents
251 in soybean accessions (**Figure 3D**). We also identified another *GST* gene, *GSTL3*,
252 which was located in chromosome 13. Two functional mutations produced three
253 haplotypes, and significant associations between the different haplotypes and
254 isoflavone content was detected for each comparison (**Figure 3E**). Based on the
255 above results, we drew a schematic diagram of the roles of candidate genes according
256 to their biological functions where we indicate that *GL3* regulates isoflavone synthesis,
257 whilst *GSTT1* and *GSTL3* participate in isoflavone transport (**Figure 3F**).

258

259 **Yield related traits and the artificial selection of *CKX3***

260 Four yield related traits (pod number per plant, seed number per plant, one hundred
261 seed weight and seed size) have a common SAL located at the ~4.0 Mb to ~4.2 Mb
262 region of chromosome 17 (**Figure 4A**). Further analysis revealed that this SAL
263 contains two tandem repeat *CKX* (cytokinin oxidase/dehydrogenase) genes named
264 *CKX3* and *CKX4*, approximately 15 kb apart from each other (**Figure 4F**).

265 We further analysed the relationship between functional mutations in *CKX3* and
266 *CKX4*. There were three non-synonymous SNPs on *CKX3* and two non-synonymous

267 SNPs on *CKX4*. As these two genes are only approximately 3 kb apart from each
268 other in the same genome region, we analysed the two genes separately as well as
269 combined as one in relation to their association with haplotypes and traits (**Figure**
270 **4B-E**). Results showed that the functional mutations can both form three haplotypes
271 for *CKX3* and *CKX4* separately, and four haplotypes for *CKX3+4* combined. For all
272 comparisons in all traits, *Haplotype 1* always showed significant differences
273 compared with the other haplotypes. The relationship between different haplotypes in
274 terms of pod or seed number per plant showed a consistent trend, while that of one
275 hundred seed weight or seed size showed a consistent but opposite trend. There was a
276 phenotypic correlation between pod number per plant and seed number per plant
277 (0.92), and between one hundred seed weight and seed size (0.67) (**Figure 4F**).
278 Furthermore, we observed that *CKX3* and *CKX4* were located in different strands of
279 the same chromosome, suggesting they are more likely to have independent functions.
280 However, we did not detect expression of *CKX4* in the subsequent qPCR validation.
281 Thus, only *CKX3* is regarded as a real candidate gene, while the role of *CKX4* need
282 further study.

283 When we compared the soybean accession information of each haplotype for the
284 four yield-related traits, we observed that most accessions with the *Haplotype 1*
285 genotype had dominant traits (lower pod or seed numbers and larger seeds and seed
286 weights), and were more associated with cultivars. The other haplotypes were mainly
287 landrace-specific haplotypes, and these accessions all belong to *Group 1*. We found
288 that *CKX3* was also located on a strong selective sweep region. This indicates that the
289 functional mutation sites in *CKX3* experienced strong directed artificial selection,
290 resulting in genotype differences and affecting yield related traits. Furthermore, we
291 compared all SAGs and selective sweep regions for all traits, and found that
292 approximately 12% of genes are located in the selected sweep regions, which have
293 experienced artificial selection (**Supplementary Table 9**). It is interesting to note that
294 of all the SAGs located in selective sweep regions, about 55% are related to yield
295 traits, 36% related to protein traits, and less than 10% are related to other traits
296 (**Figure 4G, H**).

297

298 **CYP85A2 is associated with architecture and yield traits**

299 There is one SAL on chromosome 18 which is associated with six traits including
300 plant height, main stem number, stem strength, lodging, podding habit, and seed
301 weight per plant. Interestingly, these traits include both architecture and yield related
302 traits. A cytochrome P450 family gene named *CYP85A2* is located within a 4.37 kb
303 region of this SAL (**Figure 5A, B**). The association of the *CPY85A2* gene with
304 architecture and yield traits in soybean is a novel finding. We also observed that a
305 non-synonymous mutation site *c18s55526062* is involved in producing two
306 haplotypes. The haplotype with a *CC* genotype has a dwarf plant height, a low main
307 stem node number, a high stem strength and a low lodging rate. When plants produced
308 mostly limited or semi-limited pods, their seed weight per plant was also found to
309 increase (**Figure 5C**). Phenotypically, plant height was positively correlated with
310 main stem node number (0.95), while stem strength and lodging were negatively
311 correlated (-0.81), showing a trend consistent with the genotype (**Figure 5D**). The *CC*
312 genotype of *c18s55526062* is a dominant genotype, which is useful when designing
313 an ideal plant type and increasing soybean yield.

314

315 **Different phenotypes coupled through hub gene modules form a complex**
316 **phenotype-gene network**

317 Based on in-depth exploration of the GWAS results, we observed that one trait is
318 associated with multiple genes and vice versa. At the same time, due to widespread
319 protein-level interactions between genes, a complex network was also found between
320 various phenotypes and genes. In order to explore this further, we used a functional
321 mutation-based haplotype test to screen SAGs in all SALs for all traits. We then
322 constructed a phenotype-gene network which included 34 traits and 853 SAGs
323 (**Figure 6**). At the trait level, they were divided into six categories, namely
324 architecture, colour, oil, isoflavone, protein, and yield. At the gene level, besides the
325 six categories, there emerged a mixed category with which genes associated more
326 than with any one trait category. We found that traits in the same category were

327 closely linked within the entire network. However, some trait categories were also
328 linked with each other, such as yield, oil, protein and colour, and they were all closely
329 linked to architecture through common SAGs. This suggests that there are subtle
330 relationships between architecture and other trait categories. In this genetic network,
331 six trait categories were linked through 15 hub nodes containing a total of 367 genes
332 (**Supplementary Table 10**). The largest hub was *HAI* (short form for *Hub*
333 *Architecture 1*). The genes in this hub were only associated with two or more
334 architecture-related traits. Unlike *HAI*, the genes in the *HA2* node were associated
335 with two or more architecture-related traits, but also had protein interactions with
336 other genes. Multiple yield traits were associated with hub *HYI*, containing *CKX3*,
337 while hub *HM4*, which contains *CYP85A2*, was connected with architecture and yield
338 traits.

339

340 **Discussion**

341 In this study, we deeply sequenced 250 representative landrace and cultivar soybean
342 accessions. Through population genetics and GWAS analyses, the genetic structure of
343 European soybean varieties was analysed for the first time. Novel candidate genes
344 related to seed isoflavone content, yield and architecture traits were identified.
345 Moreover, we constructed a soybean phenotype-gene interaction network, and found
346 evidence of the improvement of soybean yield related traits at molecular level.

347 A total of ~3T bases and 6M SNPs were obtained, the maximum sequencing
348 depth of a single accession was 22.5x, with the average depth at 11x (higher than
349 previous soybean resequencing studies[2-4]. Eighty-four percent of the accessions
350 with their genome were sequenced for the first time, which provides new data for
351 soybean genome research. Previous soybean research mainly focused on varieties
352 from Asia and North America, but not Europe[3, 4]. This study completed the
353 resequencing of 26 European accessions and, for the first time, outlines a breeding
354 history of European soybean. It was found that European soybean cultivars had higher
355 genetic diversities and lower breeding levels compared to North American cultivars.

356 Both European and American soybean cultivars may have been introduced from
357 different ancestors in China. This theory is based on the following findings: there is a
358 small population difference between European varieties and Chinese landraces, and
359 between American varieties and Chinese cultivars, whilst there is a large population
360 difference between American and European varieties (**Figure 2G, Supplementary**
361 **Figure 2**). Our findings are consistent with the current hypothesis that soybean
362 originated in China, and they show that ancestral components from the area of origin
363 are the most complex. This study showed that the heterozygosity rates of most
364 accessions are less than 0.2, except four accessions with a higher heterozygosity
365 which may be caused by their complex ancestral compositions (**Supplementary**
366 **Table S3**). Further combination analysis of the selective sweep and GWAS revealed
367 that artificial selection of soybean at the phenotypic level is consistent with the
368 genome level. Genomic regions associated with yield and quality traits are more
369 likely to experience artificial selection. This may be a reflection of yield- and
370 quality-directed artificial selection of soybean breeding at the genetic level.
371 Furthermore, evidence of functional mutations under artificial selection for a
372 candidate gene *CKX3* related to multiple yield traits were identified. The results of
373 this study provide valuable information for marker-assisted selection, which is vital in
374 the improvement of soybean breeding.

375 Isoflavone is a secondary metabolite produced via phenylpropane metabolic
376 pathways in higher plants. Isoflavone is associated with plant stress resistance,
377 defence against microbial and insect infection, promotion of rhizobium chemotaxis,
378 and the development of rhizome and nitrogen fixation in plants. It also provides health
379 benefits to human, such as in reducing the incidence of cancer and cardiovascular
380 diseases, and regulating the immune response[12]. Therefore, increasing the seed
381 isoflavone content of soybean can improve its nutritional and health benefits.
382 However, few genome-wide studies have investigated the molecular mechanism of
383 soybean's isoflavone content. Isoflavone is synthesized in the cytoplasm, but due to
384 cell cytotoxicity, it cannot accumulate in the cytoplasm and must be continuously
385 transported to vacuoles for storage. Therefore, isoflavone content mainly depends on

386 two factors: synthesis efficiency and transport efficiency[13]. The transcript factor
387 *GL3* is a *bHLH* gene family member which can form the MYB-bHLH-WD40 (MBW)
388 complex with two other transcription factors (*MYB* and *WD40*) to jointly regulate the
389 synthesis of flavonoids and anthocyanin in plants[14]. *GST* can bind with glutathione
390 (GSH) to form an ABC transporter to transport and catalyse the entry of flavonoids
391 into vacuoles for accumulation[13]. In this study, we identified four novel genes that
392 may be associated with isoflavone content. These genes include transcription factors
393 *GL3*, which participate in the regulation of multi-enzyme systems from
394 phenylpropanoid to isoflavone biosynthesis pathways, and two *GST* genes, *GSTT1*
395 and *GSTL3*, which facilitate the transporting of isoflavone from the cytoplasm to
396 vacuoles (**Figure 3F**). In addition, we observed many other genes in the SALs, such
397 as cation/H⁺ exchanger (*CHX20*), pyrophosphorylase 4 (*PPa4*), an actin
398 depolymerizing factor 7 (*ADF7*), a mitochondrial substrate carrier family protein, a
399 myosin heavy chain-related protein, an *ATP* synthase alpha/beta family protein, and a
400 protein kinase superfamily protein, among others (**Supplementary Table 8**) are all
401 related to isoflavone transport. This over-representation of transport-related genes
402 further suggests that the accumulation of soybean isoflavone is related to its transport
403 to the vacuole. In conclusion, soybean isoflavone content is not merely determined by
404 one or several genes or loci, but by a multiple gene system involved in synthesis,
405 regulation, transport, and storage.

406 We observed that other novel candidate genes, such as *CKX3*, is associated with
407 multiple yield traits. We also observed, for the first time, that *CYP85A2* is associated
408 with multiple architecture and yield traits in soybean. It is well-known that cytokinin
409 promotes cell division and plant growth, and *CKX* is one of the key enzymes in
410 cytokinin metabolism. A functional variation in the *CKX* gene may affect the
411 cytokinin metabolism, thus affecting grain yield and related traits. A number of
412 studies on *Arabidopsis thaliana*, rice and other crops have shown that mutation or
413 reduced expression levels of *CKX* family genes are related to a decrease in seed
414 setting rate and an increase in seed weight[15, 16]. *CYP85A2* is involved in the
415 brassinosteroid biosynthesis pathway in *Arabidopsis thaliana* and it converts

416 6-deoxocastasterone to castasterone, which is followed by the conversion of
417 castasterone to brassinolide[17]. Brassinosteroids (BRs) are broad-spectrum plant
418 growth regulators, playing an important role in plant growth and development, as well
419 as in biological and abiotic stress responses[18]. Mutations in the *CYP85A2* gene have
420 led to an increased production of the dwarf phenotype[19], and an overexpression of
421 the *CYP85A* family gene resulting in increased BR content, biomass, plant height,
422 plant fresh weight and fruit yield[20]. These results showed that, *CKX3* and *CYP85A2*
423 may affect soybean yield and architecture related traits through different molecular
424 mechanisms. The potential effect of functional mutations in these genes on the
425 phenotypes was further confirmed by our haplotype tests. However, to verify whether
426 these candidate genes and functional mutations are the true cause of the phenotypic
427 differences, further functional verification of these genes is necessary. Multiple
428 methods such as the construction of isolated populations, transgene, gene knockout,
429 gene editing, and expression verification could be used for this purpose. In this study,
430 we performed expression verification in seedlings with different
431 haplotypes/phenotypes for six genes *GL3*, *GSTL3*, *GSTT1b*, *CKX3*, *CKX4* and
432 *CYP85A2*. The results show that, except for no expression were detected for *CKX4*,
433 all the other five genes were expressed differently for different haplotypes/phenotypes
434 in seedlings; the expression levels of *GL3*, *GSTL3* and *GSTT1b* related to isoflavone
435 content in the strains with high isoflavone content values was significantly higher than
436 that in the strains with low isoflavone content values (T-test, $P < 0.05$); the expression
437 level of *CKX3* in the strains with high yield phenotype values was significantly higher
438 than that in the strains with low yield phenotype values (T-test, $P < 0.05$)
439 (**Supplementary Figure 55**).

440 The highest goal of plant breeding is to aggregate many desired traits into a
441 single genome. Breeders need to simultaneously select and improve multiple related
442 traits. However, because multiple traits are interrelated, it is possible that when
443 screening for a favourable trait one also selects an unfavourable one. Understanding
444 the genetic network behind different traits can help breeders increase breeding
445 efficiency. Although soybean genetic networks for multiple agronomic traits have

446 been established at the loci level[4], we built a new phenotype-gene network which
447 includes 34 traits and 853 genes. This network reflects the relationship between
448 phenotypes and genes more directly than the previous phenotype-SAL network, and is
449 more conducive to the discovery of important candidate genes. For example, the *Hub*
450 *Mixed 1 (HMI)* node was associated with two or more trait types (architecture, colour
451 or protein), while the *HBT* gene in the *HMI* node was associated with six architectural
452 traits (branch number, main stem number, plant height, stem strength, lodging, and
453 podding habit) and four protein-related traits (phenylalanine content, isoleucine
454 content, tyrosine content, and glycine content). It is known that the *HBT* gene belongs
455 to the *CDC27b* gene family and is involved in cell cycle regulation, which is related
456 to cell development and division[21]. Therefore, soybean architecture is likely
457 affected by *HBT*, despite its relationship with amino acid content is unclear. There are
458 also many other interesting examples of the above. Leaf shape is known to affect
459 photosynthesis efficiency, followed by carbohydrate accumulation, and, as a
460 consequence, oil accumulation, while Hub *HM2*, containing *FAD2*, connects oil
461 content and leaf shape[22]. It has also been reported that oil traits and seed coat lustre
462 traits experienced parallel selection during bean domestication[23]. The hub *HM3*
463 node connects oil-related traits and seed coat lustre. Anthocyanin synthesis and
464 isoflavone synthesis share part of their metabolic pathways and hub *HM5* connects
465 colour traits and isoflavone content. Our phenotype-gene network may surpass the
466 phenotype-SAL network in terms of candidate gene selection, which is also beneficial
467 to polymerization breeding programs. For example, breeders can achieve
468 polymerization breeding by directly selecting a favourable gene (such as *CYP85A2*) in
469 Hub *HM4*, which is related to both yield and architecture traits, and eliminate the
470 confusion of other adverse genes located in the same SAL. Furthermore, it is worth
471 noting that the architecture related traits, which centrally connect various other trait
472 categories, have the most extensive connectivity. In other words, there are numerous
473 relationships between architecture related traits and other trait categories in the
474 phenotype-gene network (**Figure 6**), suggesting that some candidate genes related to
475 architecture traits may also be related to other trait types. This may provide theoretical

476 support and practical guidance for parallel selection breeding and promote “ideotype”
477 breeding in soybean. The next step is to conduct more in-depth functional
478 investigations on genes with a potential application value, such as *CKX3* and
479 *CYP85A2*. This would help promote the design and breeding process of soybean
480 varieties with a higher yield and quality. Overall, our work is conducive to promoting
481 soybean genome functional research and genomic breeding.

482

483 **Materials and Methods**

484 **Plant materials and phenotyping**

485 A total of 250 soybean varieties were analysed in this study, which were provided by
486 the National Crop Germplasm Resources Platform, Institute of Crop Genetics,
487 Institute of Crop Sciences, Chinese Academy of Agricultural Sciences. All materials
488 were planted and phenotyped at three locations: the Gongzhuling experimental site in
489 the Jilin Academy of Agricultural Sciences (latitude 43.51°, east longitude 124.80°),
490 the Harbin experimental site in the Heilongjiang Academy of Agricultural Sciences
491 (45.68° north latitude, 126.61° east longitude), and the Chifeng experimental site un
492 the Agricultural Science Institute in Inner Mongolia (42.27° north latitude, 118.90°
493 east longitude) in late April of 2008, 2009 and 2010, respectively. Grain protein
494 content was measured using the Kjeldahl method from National Food Safety Standard
495 GB5009.5-2010 China[24], while the grain fatty acid contents were determined using
496 the Soxhlet extraction method from National Food Safety Standard GB/T5512-2008,
497 China[25]. Amino acid content was determined using high performance liquid
498 chromatography (S433D, Seckam, Germany) following a previous amino acid
499 determination method from National Food Safety Standard GB/T 18246-2000,
500 China[26]. Grain isoflavone content was determined using high performance liquid
501 chromatography from National Food Safety Standard GB/T23788-2009, China[27].
502 Finally, the phenotypic data were integrated using the BLUP (Best Linear Unbiased
503 Prediction) method using R[28] in order to remove environmental effects and obtain
504 stable genetic phenotypes. Seeds were planted in (CLC-BIV-M/CLC404-TV, MMM,

505 Germany) at 20°C (with 12-h day/12-h night) and a relative humidity of 60–80% till
506 six leaves stage (about two-week-old). Two-week-old seedlings (24°C, 12-h day/12-h
507 night cycle) were used in this qPCR validation.

508

509 **DNA preparation and sequencing**

510 The genomic DNA for all soybean accessions were extracted from soybean leaves
511 after three weeks of growth. DNA extraction was performed using the
512 cetyltrimethylammonium bromide (CTAB) method[29]. The library for each
513 accession was constructed with an insert size of approximately 500 base pairs,
514 following manufacturer's instructions (Illumina Inc., San Diego, CA, USA). All
515 soybean accessions were sequenced and paired-end 150 bp reads were produced using
516 an Illumina NovaSeq 6000 sequencer at the BerryGenomics Company
517 (<http://www.berrygenomics.com/> Beijing, China).

518

519 **Total RNA extraction, cDNA synthesis and qRT-PCR analysis**

520 Total RNA was isolated for each sample using TRIzol Reagent (Invitrogen,
521 Nottingham, UK) according to the manufacturer's instructions. The purified RNA was
522 stored at -80°C until subsequent analyses. According to the manufacturer's
523 instructions (Takara, Shiga, Japan), first-strand cDNA synthesis was performed using
524 M-MLV reverse transcriptase. Quantitative real-time PCR (qRT-PCR) was performed
525 using a SYBR Premix Ex Taq Kit (Takara) and a real-time PCR machine (CFX96;
526 Bio-Rad, Hercules, CA, USA), following the manufacturer's instructions. The
527 procedure used for qRT-PCR was 95°C at 10 minutes, followed by 38 cycles of 15 s at
528 95°C and 60 s at 61-62°C. β -actin was used as a reference gene for analysis of relative
529 expression patterns of mRNA. The reactions were carried out with three biological
530 replicates, with at least two technical replicates for each sample. The data were
531 analyzed using the method according to the previous study[30], and the means \pm
532 standard errors (SE) of three biological replicates are presented.

533

534 **Mapping, variant calling and annotation**

535 Raw paired-end resequencing reads were first cleaned by removing reads with
536 adaptors, reads of low quality and reads with “N”s. The high-quality clean reads were
537 then mapped to the soybean reference genome (Williams 82 assembly v2.1) with
538 BWA[31]. Statistical analyses of mapping rate and genomic coverage of clean reads
539 were performed using in-house scripts. The Speedseq pipeline[32] was used for SNP
540 and Indel calling, and vcftools[33] was used for genotype filtering. Missing genotypes
541 were imputed and phased through a localized haplotype clustering algorithm
542 implemented using Beagle v3.0[34]. Variant annotation was performed using
543 ANNOVAR[35] against the soybean gene model set v2.1.42. After annotation, SNPs
544 and Indels were categorized into exonic, intronic, intergenic, splicing, 5'UTRs,
545 3'UTRs, upstream, and downstream. Exonic SNPs were further categorized into
546 synonymous, nonsynonymous, stop gain, and stop loss. Exonic Indels were further
547 categorized into frameshift, non-frameshift, stop gain, and stop loss.

548

549 **Population structure analysis**

550 Approximately 6M SNPs from the 250 soybean accessions were concatenated for the
551 construction of a phylogenetic tree. Using a neighbour joining algorithm with a
552 pairwise gap deletion method for 100 bootstrap replications, a phylogenetic tree was
553 constructed with MegaCC[36]. The output was displayed using the iTOL[37] web
554 tool. With the whole genome genotype as the input, a principal component analysis
555 (PCA) was done using flashPCA [38] and the first two eigenvectors were plotted. A
556 population admixture analysis with $k = 2$ to $k = 5$ parameters were set to infer the
557 admixture of ancestors using fastSTRUCTURE.

558

559 **Genetic diversity analysis**

560 Linkage disequilibrium analyses for each subpopulation were performed using
561 PLINK[39] by calculating the correlation coefficient (r^2) of any two SNP pairs in one
562 chromosome. An LD decay plot was drawn using the average r^2 value for the distance
563 from 0 to 1,000 kb. Pairwise IBS calculations were also performed using PLINK and
564 a distance matrix was generated for each subpopulation. Population genetic diversities

565 were measured using VCFtools[33] by calculating $\theta\pi$ and Fst . $\theta\pi$ was used to measure
566 the genetic diversity of each subpopulation, while Fst , plus the allele frequency
567 distribution (AFD) plot (which was generated by in-house scripts), were used to
568 measure genetic diversity between subpopulations. In addition, sliding window
569 calculations of r^2 , $\theta\pi$, Fst and $Tajima' D$ values were also performed for genome-wide
570 displays of soybean genetic diversities with a 100 kb window and a 10 kb step.

571

572 **Selective sweep analysis**

573 We used two methods to detect selective sweep regions across the soybean genome:
574 $Tajima' D$ combined $\theta\pi$ and Fst combined $\theta\pi$ ratios. Firstly, a genome-wide sliding
575 window calculation of $\theta\pi$, Fst , and $Tajima' D$ values (with a 100 kb window and a 10
576 kb step) were performed on landraces, cultivars, and the whole population,
577 respectively. Secondly, the top 5% of the $Tajima' D$ and $\theta\pi$ windows for the whole
578 population were selected. In addition, the top 5% of the Fst and $\theta\pi$ ratio windows for
579 the landraces versus cultivars were also selected. Thirdly, the selected windows from
580 these two methods were merged together to become the final selective sweep regions.
581 ROH analyses for each accession were performed using PLINK[39] with the
582 parameters of a minimum ROH length set to 300 kb.

583

584 **GWAS and significantly associated loci**

585 Association analysis for each trait on each SNP with an MAF larger than 0.05 was
586 performed using a single-locus mixed linear model (MLM) implemented in
587 GEMMA[40] (which corrects confounding by population structure and the
588 relatedness matrix). The GWAS results were displayed using a Manhattan plot and a
589 QQ-plot created with the R package CMplot[41]. A clump based method
590 implemented in PLINK[39] was used to reduce a false peak and to detect real SALs.
591 The P-value cut-off was set to 10^{-5} so as to, firstly, uncover significant associated
592 SNPs. Following this, for each significantly associated SNP, if there were more than
593 10 SNPs within a 100 kb distance that had P-values smaller than 10^{-4} , then the region
594 was regarded as a potential SAL. Finally, all overlapping SALs were merged to

595 generate final SAL sets and the SNP with the smallest P-value in a SAL was defined
596 as a peak.

597

598 **Detection of significantly associated genes**

599 There are usually tens of genes in a SAL, and it is difficult to determine which genes
600 are truly associated with traits and which are irrelevant. We improved a functional
601 mutation-based haplotype test method for SAG discovery in SAL. As most variants
602 within a gene are non-functional, the gene's amino acid sequence and its function will
603 not change. Only a few variants have the potential to change a gene's amino acid
604 sequence, such as nonsynonymous SNPs, frameshift Indels, variants in splicing sites,
605 promoter regions, start codons, and stop codons. These combined functional
606 mutations can only produce two or three different gene haplotypes. It is possible to
607 test the relationship between gene haplotypes and traits. If they are significantly
608 associated, then the gene is also most likely associated with the trait, which is how
609 SAG is defined. In this study, Welch's test was used for a two-group haplotype test
610 and a Tukey's test was used for a multiple group haplotype test to detect SAGs.
611 Functional annotation of SAGs was directly retrieved from SoyBase[42].

612

613 **Network construction**

614 Of all the genes located in the SALs, the most significant SAGs with a P-value
615 smaller than 10^{-5} , and their corresponding traits, were retained to build the
616 phenotype-gene network for soybean. Protein-protein interaction information for
617 soybean was retrieved from the String database[43] and mapped to the soybean genes
618 using BLAST[44]. Construction, visualization and exploration of the network was
619 performed using Cytoscape[45].

620

621 **Data availability**

622 The raw sequence data reported in this paper have been deposited in the Genome
623 Sequence Archive[46] in BIG Data Center[47], Beijing Institute of Genomics (BIG),

624 Chinese Academy of Sciences, under accession numbers CRA002552 that are
625 publicly accessible at <https://bigd.big.ac.cn/gsa>. The variation data reported in this
626 paper have been deposited in the Genome Variation Map [48] under accession number
627 GVM000076 that can be publicly accessible at
628 <http://bigd.big.ac.cn/gvm/getProjectDetail?project=GVM000076>. The bioinformatics
629 analysis scripts used in this paper can be download through
630 https://github.com/yjthu/GPB_250SoyReseq.

631

632

633 **CRedit statement**

634 **Chunming Yang:** Resources, Investigation, Validation. **Jun Yan:** Methodology,
635 Formal analysis, Writing, Revision. **Shuqin Jiang:** Formal analysis. **Xia Li:**
636 Investigation, Validation. **Haowei Min:** Conceptualization, Supervision, Formal
637 analysis, Writing, Revision. **Xiangfeng Wang:** Conceptualization, Supervision,
638 Writing, Revision. **Dongyun Hao:** Conceptualization, Supervision, Writing, Revision.
639 All authors read and approved the final manuscript.

640

641 **Competing interests**

642 The authors declare no competing financial interests.

643

644 **Acknowledgements**

645 This research was supported by grants from the Agricultural Science and Technology
646 Innovation Project, Jilin Province [CXGC2017ZY027], and from Program of
647 Accurate Identification and Display of Soybean Germplasm, China
648 [NB08-2130315-(25-31)-06, NB07-2130315-(25-30)-06, NB06-070401-(22-27)-05,
649 NB2010-2130315-25-05]. We are grateful to Prof. Lijuan Qiu for her agreement of
650 using the 250 soybean varieties from her laboratory at China Academy of Agricultural
651 Sciences. We appreciate Dr. Zhangxiong Liu of China Academy of Agricultural
652 Sciences for the technical guidance in soybean phenotypic characterization.

653 Acknowledgement also goes to Yunshan Wei (Inner Mongolia Academy of Agriculture
654 & Animal Husbandry Sciences), Shuhong Wei and Qiang Wang (Heilongjiang
655 Academy of Agricultural Sciences), for partially phenotypic characterization of the
656 soybean population used in this work.

657

658 **References**

- 659 [1] Sedivy, E.J., F. Wu, and Y. Hanzawa. Soybean domestication: the origin, genetic
660 architecture and molecular bases. *New Phytol* 2017;214:539-553.
- 661 [2] Lam, H.M., X. Xu, X. Liu, W. Chen, G. Yang, F.L. Wong, et al. Resequencing of
662 31 wild and cultivated soybean genomes identifies patterns of genetic diversity
663 and selection. *Nat Genet* 2010;42:1053-9.
- 664 [3] Zhou, Z., Y. Jiang, Z. Wang, Z. Gou, J. Lyu, W. Li, et al. Resequencing 302 wild
665 and cultivated accessions identifies genes related to domestication and
666 improvement in soybean. *Nat Biotechnol* 2015;33:408-14.
- 667 [4] Fang, C., Y. Ma, S. Wu, Z. Liu, Z. Wang, R. Yang, et al. Genome-wide association
668 studies dissect the genetic networks underlying agronomical traits in soybean.
669 *Genome Biol* 2017;18:161.
- 670 [5] Schmutz, J., S.B. Cannon, J. Schlueter, J. Ma, T. Mitros, W. Nelson, et al. Genome
671 sequence of the palaeopolyploid soybean. *Nature* 2010;463:178-83.
- 672 [6] Nielsen, R. Molecular signatures of natural selection. *Annu Rev Genet*
673 2005;39:197-218.
- 674 [7] Purfield, D.C., S. McParland, E. Wall, and D.P. Berry. The distribution of runs of
675 homozygosity and selection signatures in six commercial meat sheep breeds.
676 *PLoS One* 2017;12:e0176780.
- 677 [8] Crowell, S., P. Korniliev, A. Falcao, A. Ismail, G. Gregorio, J. Mezey, et al.
678 Genome-wide association and high-resolution phenotyping link *Oryza sativa*
679 panicle traits to numerous trait-specific QTL clusters. *Nat Commun*
680 2016;7:10527.
- 681 [9] Yano, K., E. Yamamoto, K. Aya, H. Takeuchi, P.C. Lo, L. Hu, et al. Genome-wide
682 association study using whole-genome sequencing rapidly identifies new
683 genes influencing agronomic traits in rice. *Nat Genet* 2016;48:927-34.
- 684 [10] Meng, S., J. He, T. Zhao, G. Xing, Y. Li, S. Yang, et al. Detecting the QTL-allele
685 system of seed isoflavone content in Chinese soybean landrace population for
686 optimal cross design and gene system exploration. *Theor Appl Genet*
687 2016;129:1557-76.
- 688 [11] Zhang, J., X. Wang, Y. Lu, S.J. Bhusal, Q. Song, P.B. Cregan, et al.
689 Genome-wide Scan for Seed Composition Provides Insights into Soybean
690 Quality Improvement and the Impacts of Domestication and Breeding. *Mol*
691 *Plant* 2018;11:460-472.
- 692 [12] Messina, M. A brief historical overview of the past two decades of soy and
693 isoflavone research. *J Nutr* 2010;140:1350S-4S.

- 694 [13] Braidot, E., M. Zancani, E. Petrusa, C. Peresson, A. Bertolini, S. Patui, et al.
695 Transport and accumulation of flavonoids in grapevine (*Vitis vinifera* L.).
696 *Plant Signal Behav* 2008;3:626-32.
- 697 [14] Xu, W., C. Dubos, and L. Lepiniec. Transcriptional control of flavonoid
698 biosynthesis by MYB-bHLH-WDR complexes. *Trends Plant Sci*
699 2015;20:176-85.
- 700 [15] Li, J., X. Nie, J.L. Tan, and F. Berger. Integration of epigenetic and genetic
701 controls of seed size by cytokinin in *Arabidopsis*. *Proc Natl Acad Sci U S A*
702 2013;110:15479-84.
- 703 [16] Ashikari, M., H. Sakakibara, S. Lin, T. Yamamoto, T. Takashi, A. Nishimura, et al.
704 Cytokinin oxidase regulates rice grain production. *Science* 2005;309:741-5.
- 705 [17] Kim, T.W., J.Y. Hwang, Y.S. Kim, S.H. Joo, S.C. Chang, J.S. Lee, et al.
706 *Arabidopsis* CYP85A2, a cytochrome P450, mediates the Baeyer-Villiger
707 oxidation of castasterone to brassinolide in brassinosteroid biosynthesis. *Plant*
708 *Cell* 2005;17:2397-412.
- 709 [18] De Bruyne, L., M. Hofte, and D. De Vleeschauwer. Connecting growth and
710 defense: the emerging roles of brassinosteroids and gibberellins in plant innate
711 immunity. *Mol Plant* 2014;7:943-959.
- 712 [19] Kwon, M.F., Shozo & Ji, H.J. & Kim, Ho Bang & Takatsuto, Suguru & Yoshida,
713 Shigeo & An, Chung & Choe, Sunghwa. A double mutant for the CYP85A1
714 and CYP85A2 genes of *Arabidopsis* exhibits a brassinosteroid dwarf
715 phenotype. *Journal of Plant Biology* 2005;48:237-244.
- 716 [20] Northey, J.G., S. Liang, M. Jamshed, S. Deb, E. Foo, J.B. Reid, et al.
717 Farnesylation mediates brassinosteroid biosynthesis to regulate abscisic acid
718 responses. *Nat Plants* 2016;2:16114.
- 719 [21] Perez-Perez, J.M., O. Serralbo, M. Vanstraelen, C. Gonzalez, M.C. Criqui, P.
720 Genschik, et al. Specialization of CDC27 function in the *Arabidopsis thaliana*
721 anaphase-promoting complex (APC/C). *Plant J* 2008;53:78-89.
- 722 [22] Dar, A.A., A.R. Choudhury, P.K. Kancharla, and N. Arumugam. The FAD2 Gene
723 in Plants: Occurrence, Regulation, and Role. *Front Plant Sci* 2017;8:1789.
- 724 [23] Zhang, D., L. Sun, S. Li, W. Wang, Y. Ding, S.A. Swarm, et al. Elevation of
725 soybean seed oil content through selection for seed coat shininess. *Nat Plants*
726 2018;4:30-35.
- 727 [24] GB/T 5009.5-2010 National food safety standard Determination of protein in
728 foods.
- 729 [25] GB/T 5512-2008 Inspect of grain and oilseeds—Determination of crude fat
730 content in grain.
- 731 [26] GB/T 18246-2000 Determination of amino acids in feeds.
- 732 [27] GB/T 23788-2009 Determination of soybean isoflavone in health-care
733 food-High-performance liquid chromatography.
- 734 [28] Liu X., Rong J., Liu X. Best linear unbiased prediction for linear combinations in
735 general mixed linear models. *Journal of Multivariate Analysis* 2008;99 (8):
736 1503–1517.
- 737 [29] Murray, M.G. and W.F. Thompson. Rapid isolation of high molecular weight

- 738 plant DNA. *Nucleic Acids Res* 1980;8:4321-5.
- 739 [30] Livak, K.J. and T.D. Schmittgen. Analysis of relative gene expression data using
740 real-time quantitative PCR and the 2(-Delta Delta C(T)) Method. *Methods*
741 2001;25:402-8.
- 742 [31] Li, H. and R. Durbin. Fast and accurate long-read alignment with
743 Burrows-Wheeler transform. *Bioinformatics* 2010;26:589-95.
- 744 [32] Chiang, C., R.M. Layer, G.G. Faust, M.R. Lindberg, D.B. Rose, E.P. Garrison, et
745 al. SpeedSeq: ultra-fast personal genome analysis and interpretation. *Nat*
746 *Methods* 2015;12:966-8.
- 747 [33] Danecek, P., A. Auton, G. Abecasis, C.A. Albers, E. Banks, M.A. DePristo, et al.
748 The variant call format and VCFtools. *Bioinformatics* 2011;27:2156-8.
- 749 [34] Browning, S.R. and B.L. Browning. Rapid and accurate haplotype phasing and
750 missing-data inference for whole-genome association studies by use of
751 localized haplotype clustering. *Am J Hum Genet* 2007;81:1084-97.
- 752 [35] Wang, K., M. Li, and H. Hakonarson. ANNOVAR: functional annotation of
753 genetic variants from high-throughput sequencing data. *Nucleic Acids Res*
754 2010;38:e164.
- 755 [36] Kumar, S., G. Stecher, D. Peterson, and K. Tamura. MEGA-CC: computing core
756 of molecular evolutionary genetics analysis program for automated and
757 iterative data analysis. *Bioinformatics* 2012;28:2685-6.
- 758 [37] Letunic, I. and P. Bork. Interactive Tree Of Life (iTOL) v4: recent updates and
759 new developments. *Nucleic Acids Res* 2019;47:W256-W259.
- 760 [38] Abraham, G. and M. Inouye. Fast principal component analysis of large-scale
761 genome-wide data. *PLoS One* 2014;9:e93766.
- 762 [39] Chang, C.C., C.C. Chow, L.C. Tellier, S. Vattikuti, S.M. Purcell, and J.J. Lee.
763 Second-generation PLINK: rising to the challenge of larger and richer datasets.
764 *Gigascience* 2015;4:7.
- 765 [40] Zhou, X. and M. Stephens. Genome-wide efficient mixed-model analysis for
766 association studies. *Nat Genet* 2012;44:821-4.
- 767 [41] Yin L., Zhang H., Tang Z., Xu J., Yin D., Zhang Z., Yuan X., Zhu M., Zhao S., Li
768 X. et al. rMVP: A Memory-efficient, Visualization-enhanced, and
769 Parallel-accelerated tool for Genome-Wide Association Study. *bioRxiv* 2020;
770 doi:10.1101/2020.08.20.258491.
- 771 [42] Grant, D., R.T. Nelson, S.B. Cannon, and R.C. Shoemaker. SoyBase, the
772 USDA-ARS soybean genetics and genomics database. *Nucleic Acids Res*
773 2010;38:D843-6.
- 774 [43] Szklarczyk, D., J.H. Morris, H. Cook, M. Kuhn, S. Wyder, M. Simonovic, et al.
775 The STRING database in 2017: quality-controlled protein-protein association
776 networks, made broadly accessible. *Nucleic Acids Res* 2017;45:D362-D368.
- 777 [44] Madden, T. The BLAST sequence analysis tool. *The NCBI Handbook* [Internet].
778 2nd edition 2013;
- 779 [45] Shannon, P., A. Markiel, O. Ozier, N.S. Baliga, J.T. Wang, D. Ramage, et al.
780 Cytoscape: a software environment for integrated models of biomolecular
781 interaction networks. *Genome Res* 2003;13:2498-504.

- 782 [46] Wang, Y., F. Song, J. Zhu, S. Zhang, Y. Yang, T. Chen, et al. GSA: Genome
783 Sequence Archive<sup/>. Genomics Proteomics Bioinformatics
784 2017;15:14-18.
- 785 [47] National Genomics Data Center, M. and Partners. Database Resources of the
786 National Genomics Data Center in 2020. Nucleic Acids Res
787 2020;48:D24-D33.
- 788 [48] Song, S., D. Tian, C. Li, B. Tang, L. Dong, J. Xiao, et al. Genome Variation Map:
789 a data repository of genome variations in BIG Data Center. Nucleic Acids Res
790 2018;46:D944-D949.

791

792

793

794

795

796

797

798

799

800

801 Tables

802 **Table1.** Functional variants of representative significant associated genes

| Variant ID | Chrom | Positon | Ref | Alt | Variant type | Gene ID | Gene symbol |
|--------------|-------|----------|-----|-----|-------------------|-----------------|---------------|
| c5s38936266 | 5 | 38936266 | C | T | nonsynonymous SNV | GLYMA_05G206900 | <i>GSTT1a</i> |
| c5s38940717 | 5 | 38940717 | C | T | nonsynonymous SNV | GLYMA_05G207000 | <i>GSTT1b</i> |
| c5s39035509 | 5 | 39035509 | G | C | nonsynonymous SNV | GLYMA_05G208300 | <i>GL3</i> |
| c5s39036346 | 5 | 39036346 | T | C | nonsynonymous SNV | GLYMA_05G208300 | <i>GL3</i> |
| c13s24804891 | 13 | 24804891 | C | T | nonsynonymous SNV | GLYMA_13G135600 | <i>GSTL3</i> |
| c13s24805363 | 13 | 24805363 | A | T | splicing SNV | GLYMA_13G135600 | <i>GSTL3</i> |
| c17s4143663 | 17 | 4143663 | C | T | nonsynonymous SNV | GLYMA_17G054500 | <i>CKX3</i> |
| c17s4143832 | 17 | 4143832 | T | C | nonsynonymous SNV | GLYMA_17G054500 | <i>CKX3</i> |
| c17s4146922 | 17 | 4146922 | G | T | nonsynonymous SNV | GLYMA_17G054500 | <i>CKX3</i> |

| | | | | | | | |
|--------------|----|----------|---|---|-------------------|-----------------|----------------|
| c17s4151713 | 17 | 4151713 | C | A | nonsynonymous SNV | GLYMA_17G054600 | <i>CKX4</i> |
| c17s4151752 | 17 | 4151752 | T | C | nonsynonymous SNV | GLYMA_17G054600 | <i>CKX4</i> |
| c18s55526062 | 18 | 55526062 | C | T | nonsynonymous SNV | GLYMA_18G272300 | <i>CYP85A2</i> |

803

804

805

806

807

808

809

810

811

812

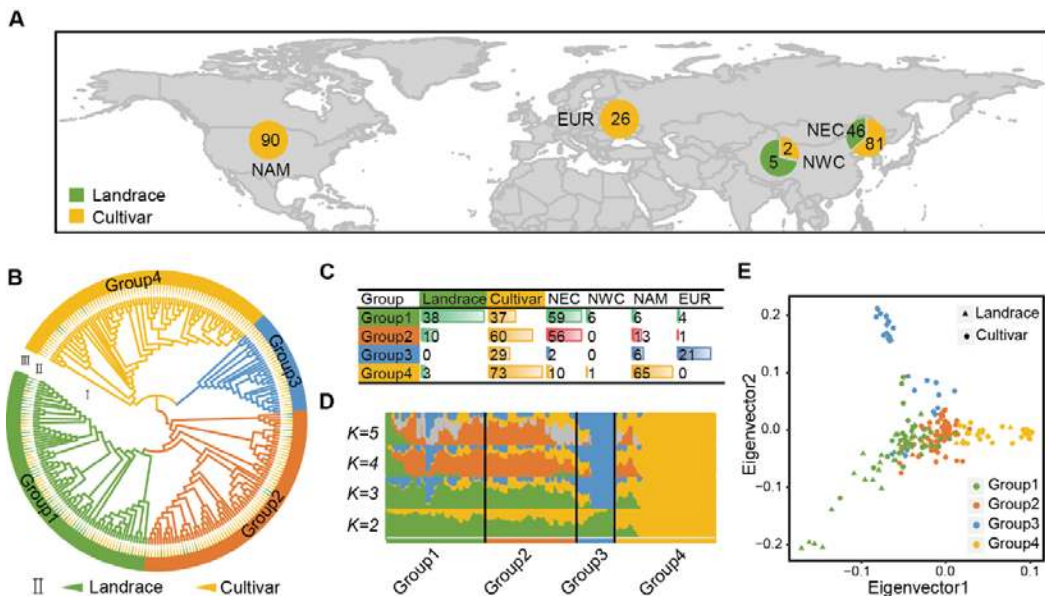
813

814

815 **Figures**

816

817 **Figure 1**



818

819 **Figure 1** Population structure of 250 soybean accessions. **A.** Geographic distribution
 820 of 250 soybean landraces and cultivars. Landraces are shown with green color and
 821 cultivars are shown with yellow color. **B.** Phylogenetic tree constructed for all
 822 soybean accessions. Group1-4 are shown with different colors, Landraces are labeled
 823 with green triangles and cultivars are labeled with yellow triangles. **C.** Statistics of the
 824 geographic origin for each subpopulation. **D.** Mixed ancestors analysis for soybean
 825 subpopulations. Each color represents an ancestral component. K from 2 to 5 are set
 826 to trace different ancestral components. **E.** PCA plot of the first two eigenvectors for
 827 all soybean accessions. Landraces and cultivars are shown with different shape, while
 828 groups are shown with different colors.

829

830

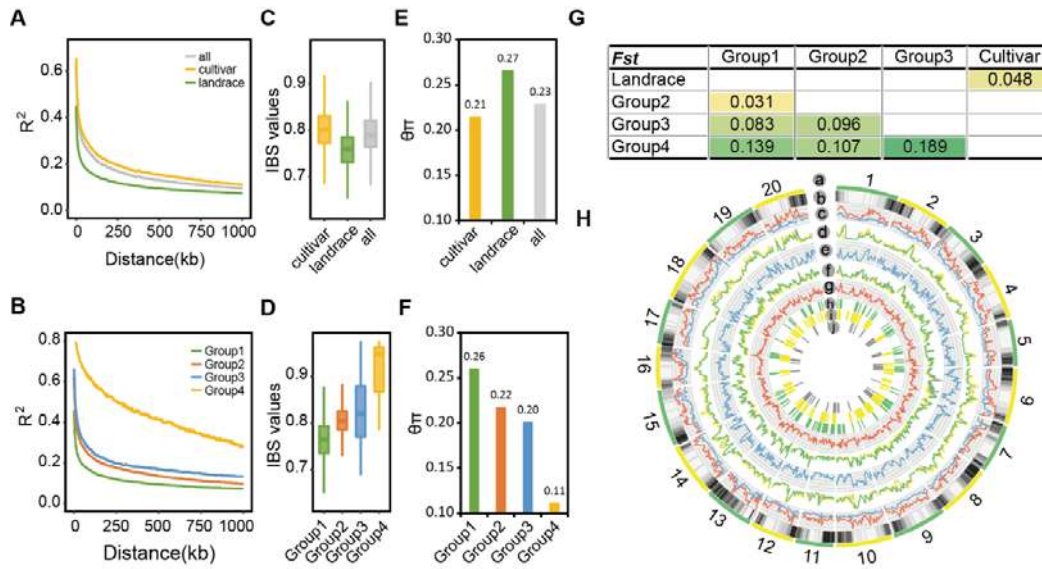
831

832

833

834

835 **Figure 2**



836

837 **Figure 2** Genetic diversity of soybean subpopulations. **A.** LD decay plots for landrace
 838 (green), cultivars (yellow) and all soybean accessions (grey). **B.** LD decay plots for
 839 soybean subpopulations. **C.** IBS values distribution for landrace (green), cultivars
 840 (yellow) and all soybean accessions (grey). **D.** IBS values distribution for soybean
 841 subpopulations. **E.** Comparison of $\theta\pi$ values for landrace (green), cultivars (yellow)
 842 and all soybean accessions (grey). **F.** Comparison of $\theta\pi$ values for soybean
 843 subpopulations. **G.** Comparison of F_{st} values between subpopulations. **H.** Landscape
 844 of soybean genetic diversity across the whole genome. (a) Chromosomes. (b) Density
 845 of genes (c) Density of SNPs (red) and Indels (blue). (d) LD values distribution for
 846 landraces (green), cultivars (yellow) and all accessions (grey). (e) F_{st} values
 847 distribution of landraces versus cultivars (f) $\theta\pi$ values distribution for
 848 landraces (green), cultivars (yellow) and all accessions (grey). (g) $Tajima'D$ values
 849 distribution of all accessions. (h) Putative selective sweep regions detected by
 850 $Tajima'D$ combine $\theta\pi$. (i) Putative selective sweep regions detected by F_{st} combine
 851 $\theta\pi$ ratios. (j) ROH region larger than 300 Kb.

852

853

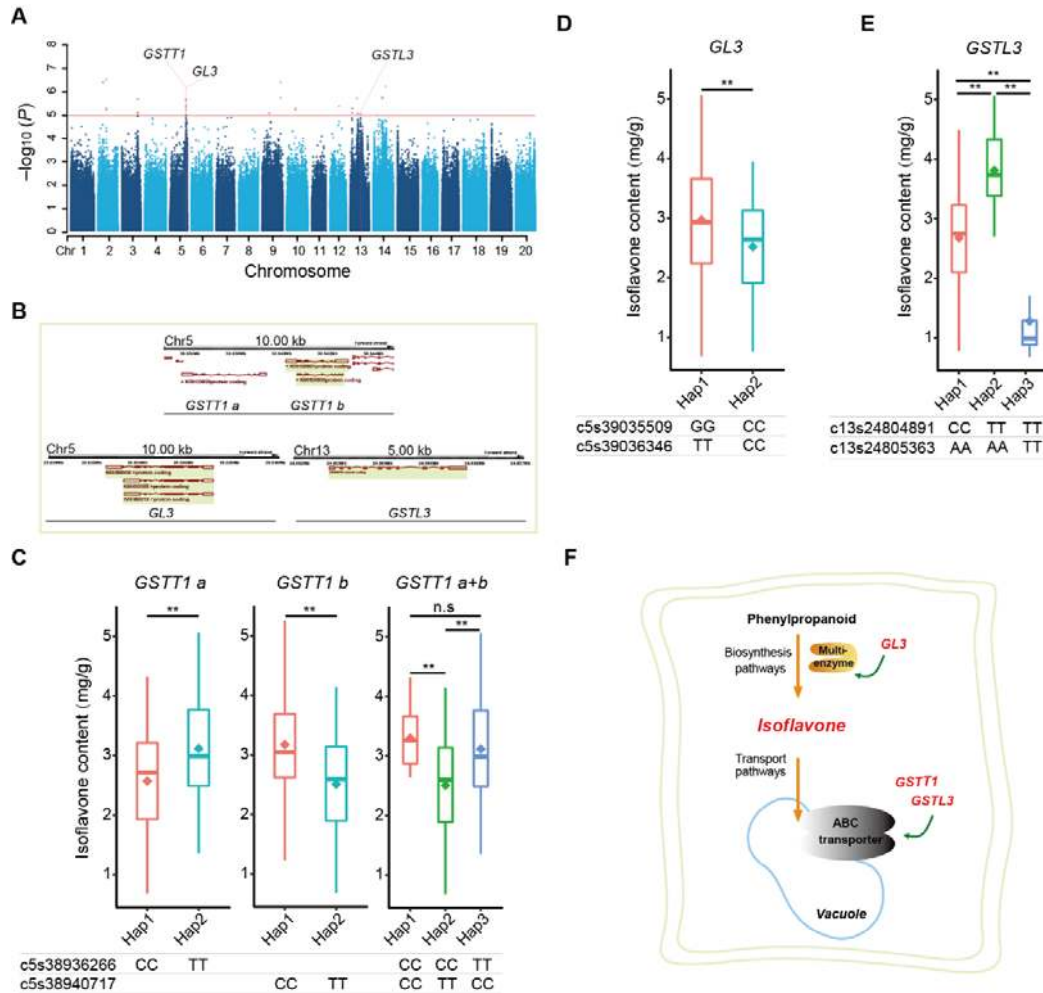
854

855

856

857 **Figure 3**

858



859

860 **Figure 3** GWAS of soybean isoflavone content. **A.** Manhantan plot and four candidate

861 genes for soybean isoflavone content. **B.** Chromosome location and transcripts

862 structure of the candidate genes. **C.** Soybean isoflavone content distribution for the

863 haplotypes of gene *GSTT1*. **D.** Soybean isoflavone content distribution for the

864 haplotypes of gene *GL3*. **E.** Soybean isoflavone content distribution for the

865 haplotypes of gene *GSTL3*. **F.** Diagram of soybean isoflavone synthesis and transport,

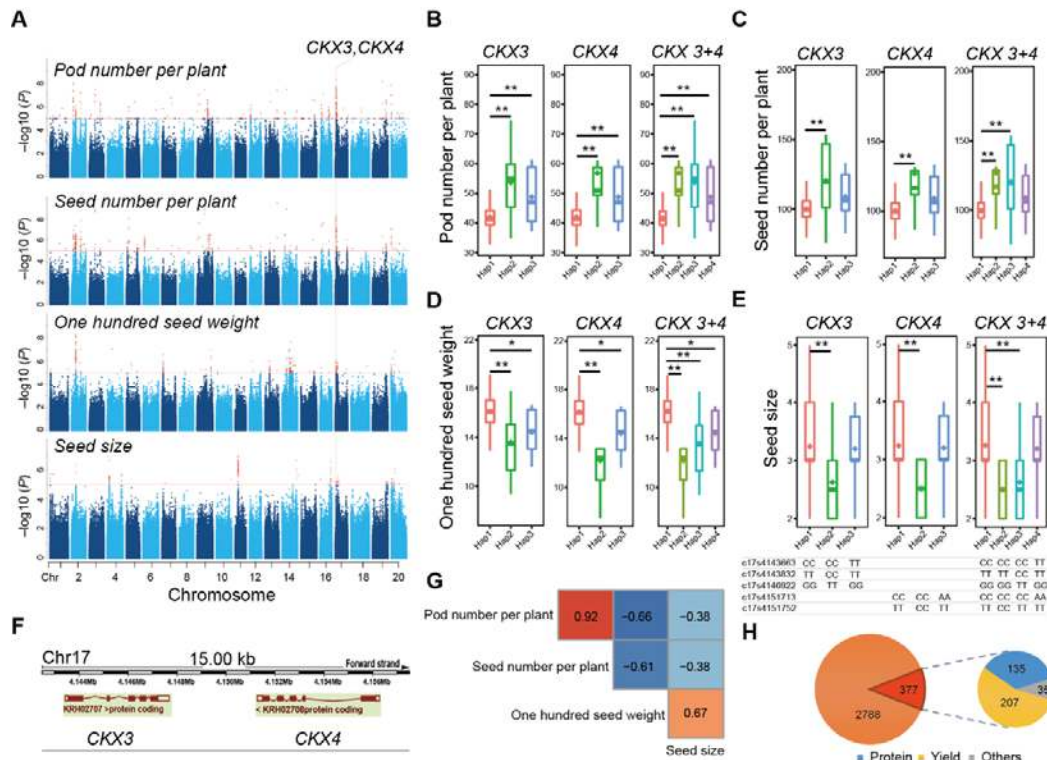
866 and the roles of candidate genes detected by GWAS. (* $P < 0.05$; ** $P < 0.01$; n.s., not

867 significant)

868

870 **Figure 4**

871



872

873 **Figure 4** Association of *CKX* and yield related traits in soybean. **A.** Manhantan plot

874 of four yield related traits pod number per plant, seed number per plant, one hundred

875 seed weight and seed size, and the candidate *CKX* genes. **B.** Pod number per plant

876 distribution for the haplotypes of *CKX* genes. **C.** Seed number per plant distribution

877 for the haplotypes of *CKX* genes. **D.** One hundred seed weight distribution for the

878 haplotypes of *CKX* genes. **E.** Seed size distribution for the haplotypes of *CKX* genes.

879 **F.** Chromosome location and transcripts structure of *CKX3* and *CKX4*. **G.** Phenotype

880 correlation of four traits. **H.** Statistics of SAGs located in selective sweep regions and

881 their percentage for trait categories. (* $P < 0.05$; ** $P < 0.01$)

882

883

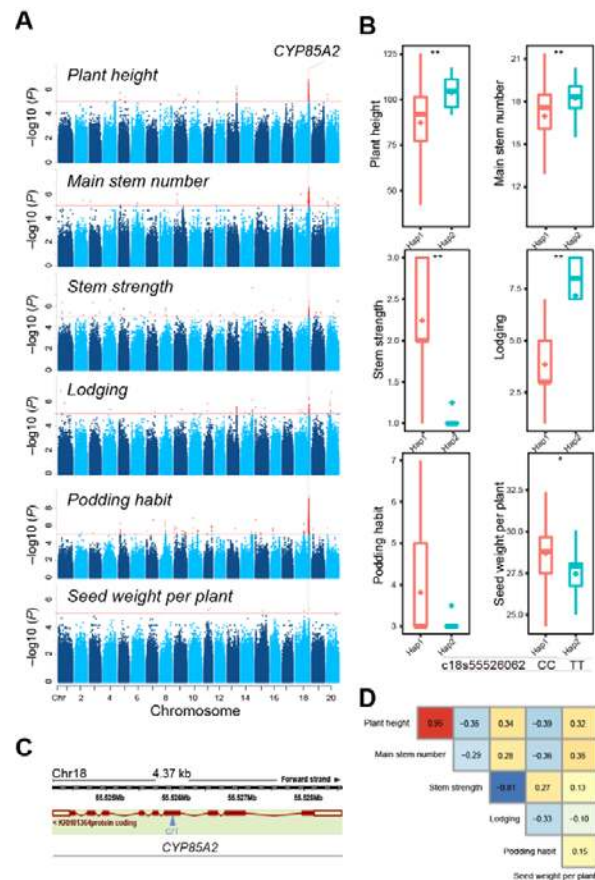
884

885

886

887 **Figure 5**

888



889

890 **Figure 5** Association of *CYP85A2* and architecture or yield related traits in soybean.

891 **A.** Manhantan plot of plant height, main stem number, stem strength, lodging,

892 podding habit, seed weight per plant, and the candidate gene *CYP85A2*. **B.** Traits

893 distribution for the haplotypes of gene *CYP85A2*. **C.** Chromosome location and

894 transcripts structure of *CYP85A2*. **D.** Phenotype correlation of the six traits. (* $P <$

895 0.05; ** $P <$ 0.01)

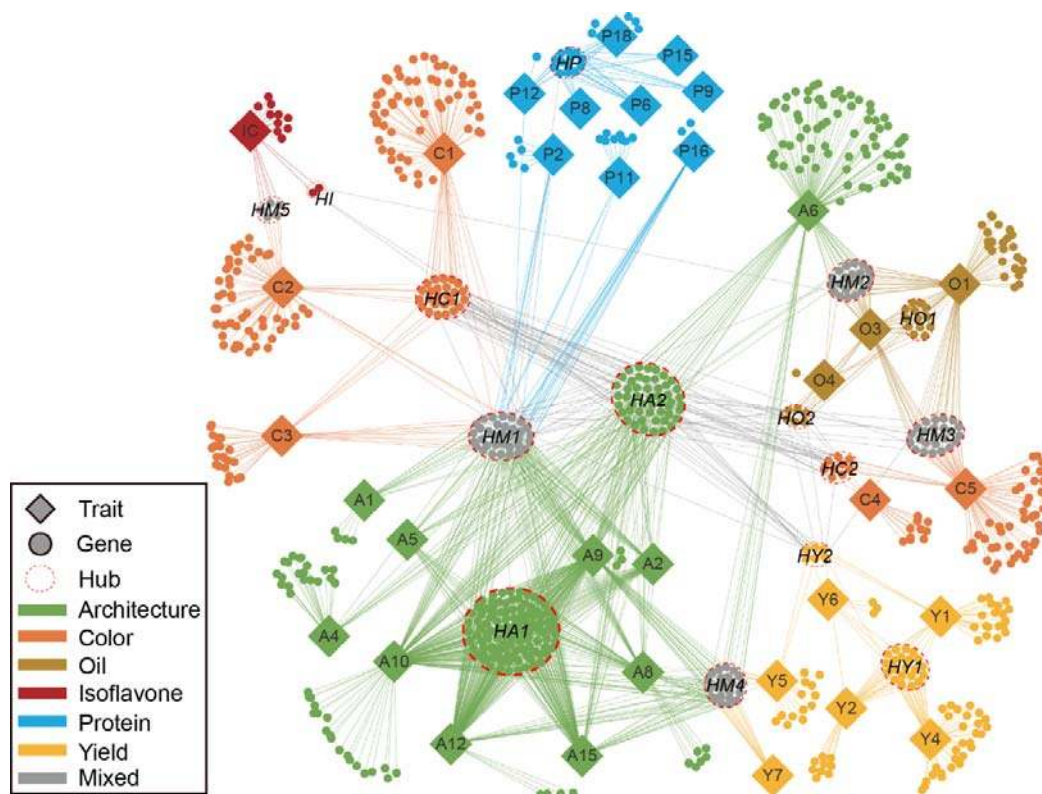
896

897

898

899 **Figure 6**

900



902 **Figure 6** Phenotype-gene genetic network in soybean. Traits are solid rhombuses,
903 genes are solid circles, and hubs are hollow ellipses. Six trait categories, their
904 associated genes and links between them are colored accordingly, genes associated
905 with more than one trait categories are colored grey. Genes with protein-protein
906 interaction are linked with gray lines.

907

908

909

910

911

912

913

914

915

916 **Supplementary material**

917 Supplementary Tables 1-10; Supplementary Figures 1-55.

918

919 **Supplementary Table 1** Summary of mapping and coverage

920 **Supplementary Table 2** Summary of SNPs and Indels

921 **Supplementary Table 3** The ancestry proportion estimates for each accession

922 **Supplementary Table 4** Putative regions experiencing selective sweeps

923 **Supplementary Table 5** Summary of ROH regions in soybean varieties

924 **Supplementary Table 6** Information of 50 agronomic traits

925 **Supplementary Table 7** Summary of significant associated loci detected by GWAS

926 analysis

927 **Supplementary Table 8** Genes located in significant associated loci for isoflavone

928 content

929 **Supplementary Table 9** Genes located in both significant associated loci and putative

930 selective sweep regions

931 **Supplementary Table 10** Summary of hub genes in soybean agronomic traits

932 networks

933

934 **Figure S1** SNP density distribution across soybean chromosomes.

935 **Figure S2** Allele frequency distribution between soybean subpopulations.

936 **Figure S3** Selective sweep analysis for 250 soybean accessions. **A.** Selective sweep

937 analysis by *Tajima*'*D* combine $\theta\pi$. **B.** Selective sweep analysis by *Fst* combine $\theta\pi$

938 ratios. Red dots present the top 5% selected windows. **C.** Venn diagram of genes

939 screened by two selective sweep analysis methods. **D.** Venn diagram of genes

940 screened by two selective sweep analysis methods and ROH analysis.

941 **Figure S4** Phenotype correlations between 50 soybean traits.

942 **Figure S5** GWAS of pod height at bottom using MLM. **A.** Density distribution of pod
943 height at bottom. **B.** Manhattan plots for pod height at bottom. Negative log₁₀
944 P-values from a genome-wide scan are plotted against SNP positions of 20
945 chromosomes. **C.** Quantile-quantile plot for pod height at bottom. The horizontal red
946 line indicates the significant threshold (10^{-5}). Trait-associated SNPs above the
947 significant threshold are colored in red.

948 **Figure S6** GWAS of effective branch number using MLM. **A.** Density distribution of
949 effective branch number. **B.** Manhattan plots for effective branch number. Negative
950 log₁₀ P-values from a genome-wide scan are plotted against SNP positions of 20
951 chromosomes. **C.** Quantile-quantile plot for effective branch number. The horizontal
952 red line indicates the significant threshold (10^{-5}). Trait-associated SNPs above the
953 significant threshold are colored in red.

954 **Figure S7** GWAS of pubescence density using MLM. **A.** Density distribution of
955 pubescence density. **B.** Manhattan plots for pubescence density. Negative log₁₀
956 P-values from a genome-wide scan are plotted against SNP positions of 20
957 chromosomes. **C.** Quantile-quantile plot for pubescence density. The horizontal red
958 line indicates the significant threshold (10^{-5}). Trait-associated SNPs above the
959 significant threshold are colored in red.

960 **Figure S8** GWAS of defoliation using MLM. **A.** Density distribution of defoliation. **B.**
961 Manhattan plots for defoliation. Negative log₁₀ P-values from a genome-wide scan are
962 plotted against SNP positions of 20 chromosomes. **C.** Quantile-quantile plot for
963 defoliation. The horizontal red line indicates the significant threshold (10^{-5}).

964 Trait-associated SNPs above the significant threshold are colored in red.

965 **Figure S9** GWAS of inflorescence length using MLM. **A.** Density distribution of
966 inflorescence length. **B.** Manhattan plots for inflorescence length. Negative \log_{10}
967 P-values from a genome-wide scan are plotted against SNP positions of 20
968 chromosomes. **C.** Quantile-quantile plot for inflorescence length. The horizontal red
969 line indicates the significant threshold (10^{-5}). Trait-associated SNPs above the
970 significant threshold are colored in red.

971 **Figure S10** GWAS of leaf shape using MLM. **A.** Density distribution of leaf shape. **B.**
972 Manhattan plots for leaf shape. Negative \log_{10} P-values from a genome-wide scan are
973 plotted against SNP positions of 20 chromosomes. **C.** Quantile-quantile plot for leaf
974 shape. The horizontal red line indicates the significant threshold (10^{-5}).
975 Trait-associated SNPs above the significant threshold are colored in red.

976 **Figure S11** GWAS of leaflet size using MLM. **A.** Density distribution of leaflet size.
977 **B.** Manhattan plots for leaflet size. Negative \log_{10} P-values from a genome-wide scan
978 are plotted against SNP positions of 20 chromosomes. **C.** Quantile-quantile plot for
979 leaflet size. The horizontal red line indicates the significant threshold (10^{-5}).
980 Trait-associated SNPs above the significant threshold are colored in red.

981 **Figure S12** GWAS of lodging using MLM. **A.** Density distribution of lodging. **B.**
982 Manhattan plots for lodging. Negative \log_{10} P-values from a genome-wide scan are
983 plotted against SNP positions of 20 chromosomes. **C.** Quantile-quantile plot for
984 lodging. The horizontal red line indicates the significant threshold (10^{-5}).
985 Trait-associated SNPs above the significant threshold are colored in red.

986 **Figure S13** GWAS of number of nodes on main stem using MLM. **A.** Density
987 distribution of number of nodes on main stem. **B.** Manhattan plots for number of
988 nodes on main stem. Negative \log_{10} P-values from a genome-wide scan are plotted
989 against SNP positions of 20 chromosomes. **C.** Quantile-quantile plot for number of
990 nodes on main stem. The horizontal red line indicates the significant threshold (10^{-5}).
991 Trait-associated SNPs above the significant threshold are colored in red.

992 **Figure S14** GWAS of plant height using MLM. **A.** Density distribution of plant
993 height. **B.** Manhattan plots for plant height. Negative \log_{10} P-values from a
994 genome-wide scan are plotted against SNP positions of 20 chromosomes. **C.**
995 Quantile-quantile plot for plant height. The horizontal red line indicates the significant
996 threshold (10^{-5}). Trait-associated SNPs above the significant threshold are colored in
997 red.

998 **Figure S15** GWAS of plant type using MLM. **A.** Density distribution of plant type. **B.**
999 Manhattan plots for plant type. Negative \log_{10} P-values from a genome-wide scan are
1000 plotted against SNP positions of 20 chromosomes. **C.** Quantile-quantile plot for plant
1001 type. The horizontal red line indicates the significant threshold (10^{-5}). Trait-associated
1002 SNPs above the significant threshold are colored in red.

1003 **Figure S16** GWAS of stem termination using MLM. **A.** Density distribution of
1004 podding habit. **B.** Manhattan plots for stem termination. Negative \log_{10} P-values from
1005 a genome-wide scan are plotted against SNP positions of 20 chromosomes. **C.**
1006 Quantile-quantile plot for stem termination. The horizontal red line indicates the
1007 significant threshold (10^{-5}). Trait-associated SNPs above the significant threshold are

1008 colored in red.

1009 **Figure S17** GWAS of seed crack using MLM. **A.** Density distribution of seed crack.

1010 **B.** Manhattan plots for seed crack. Negative \log_{10} P-values from a genome-wide scan

1011 are plotted against SNP positions of 20 chromosomes. **C.** Quantile-quantile plot for

1012 seed crack. The horizontal red line indicates the significant threshold (10^{-5}).

1013 Trait-associated SNPs above the significant threshold are colored in red.

1014 **Figure S18** GWAS of stem diameter using MLM. **A.** Density distribution of stem

1015 diameter. **B.** Manhattan plots for stem diameter. Negative \log_{10} P-values from a

1016 genome-wide scan are plotted against SNP positions of 20 chromosomes. **C.**

1017 Quantile-quantile plot for stem diameter. The horizontal red line indicates the

1018 significant threshold (10^{-5}). Trait-associated SNPs above the significant threshold are

1019 colored in red.

1020 **Figure S19** GWAS of stem intension using MLM. **A.** Density distribution of stem

1021 intension. **B.** Manhattan plots for stem intension. Negative \log_{10} P-values from a

1022 genome-wide scan are plotted against SNP positions of 20 chromosomes. **C.**

1023 Quantile-quantile plot for stem intension. The horizontal red line indicates the

1024 significant threshold (10^{-5}). Trait-associated SNPs above the significant threshold are

1025 colored in red.

1026 **Figure S20** GWAS of pubescence color using MLM. **A.** Density distribution of

1027 pubescence color. **B.** Manhattan plots for pubescence color. Negative \log_{10} P-values

1028 from a genome-wide scan are plotted against SNP positions of 20 chromosomes. **C.**

1029 Quantile-quantile plot for pubescence color. The horizontal red line indicates the

1030 significant threshold (10^{-5}). Trait-associated SNPs above the significant threshold are
1031 colored in red.

1032 **Figure S21** GWAS of flower color using MLM. **A.** Density distribution of flower
1033 color. **B.** Manhattan plots for flower color. Negative \log_{10} P-values from a
1034 genome-wide scan are plotted against SNP positions of 20 chromosomes. **C.**
1035 Quantile-quantile plot for flower color. The horizontal red line indicates the
1036 significant threshold (10^{-5}). Trait-associated SNPs above the significant threshold are
1037 colored in red.

1038 **Figure S22** GWAS of leaf color using MLM. **A.** Density distribution of leaf color. **B.**
1039 Manhattan plots for leaf color. Negative \log_{10} P-values from a genome-wide scan are
1040 plotted against SNP positions of 20 chromosomes. **C.** Quantile-quantile plot for leaf
1041 color. The horizontal red line indicates the significant threshold (10^{-5}).
1042 Trait-associated SNPs above the significant threshold are colored in red.

1043 **Figure S23** GWAS of mature pod color using MLM. **A.** Density distribution of
1044 mature pod color. **B.** Manhattan plots for mature pod color. Negative \log_{10} P-values
1045 from a genome-wide scan are plotted against SNP positions of 20 chromosomes. **C.**
1046 Quantile-quantile plot for mature pod color. The horizontal red line indicates the
1047 significant threshold (10^{-5}). Trait-associated SNPs above the significant threshold are
1048 colored in red.

1049 **Figure S24** GWAS of seed coat luster using MLM. **A.** Density distribution of seed
1050 coat luster. **B.** Manhattan plots for seed coat luster. Negative \log_{10} P-values from a
1051 genome-wide scan are plotted against SNP positions of 20 chromosomes. **C.**

1052 Quantile-quantile plot for seed coat luster. The horizontal red line indicates the
1053 significant threshold (10^{-5}). Trait-associated SNPs above the significant threshold are
1054 colored in red.

1055 **Figure S25** GWAS of isoflavone content using MLM. **A.** Density distribution of
1056 isoflavone content. **B.** Manhattan plots for isoflavone content. Negative \log_{10} P-values
1057 from a genome-wide scan are plotted against SNP positions of 20 chromosomes. **C.**
1058 Quantile-quantile plot for isoflavone content. The horizontal red line indicates the
1059 significant threshold (10^{-5}). Trait-associated SNPs above the significant threshold are
1060 colored in red.

1061 **Figure S26** GWAS of linoleic acid content using MLM. **A.** Density distribution of
1062 linoleic acid content. **B.** Manhattan plots for linoleic acid content. Negative \log_{10}
1063 P-values from a genome-wide scan are plotted against SNP positions of 20
1064 chromosomes. **C.** Quantile-quantile plot for linoleic acid content. The horizontal red
1065 line indicates the significant threshold (10^{-5}). Trait-associated SNPs above the
1066 significant threshold are colored in red.

1067 **Figure S27** GWAS of linolenic acid content using MLM. **A.** Density distribution of
1068 linolenic acid content. **B.** Manhattan plots for linolenic acid content. Negative \log_{10}
1069 P-values from a genome-wide scan are plotted against SNP positions of 20
1070 chromosomes. **C.** Quantile-quantile plot for linolenic acid content. The horizontal red
1071 line indicates the significant threshold (10^{-5}). Trait-associated SNPs above the
1072 significant threshold are colored in red.

1073 **Figure S28** GWAS of oleic acid content using MLM. **A.** Density distribution of oleic

1074 acid content. **B.** Manhattan plots for oleic acid content. Negative \log_{10} P-values from a
1075 genome-wide scan are plotted against SNP positions of 20 chromosomes. **C.**
1076 Quantile-quantile plot for oleic acid content. The horizontal red line indicates the
1077 significant threshold (10^{-5}). Trait-associated SNPs above the significant threshold are
1078 colored in red.

1079 **Figure S29** GWAS of palmitic acid content using MLM. **A.** Density distribution of
1080 palmitic acid content. **B.** Manhattan plots for palmitic acid content. Negative \log_{10}
1081 P-values from a genome-wide scan are plotted against SNP positions of 20
1082 chromosomes. **C.** Quantile-quantile plot for palmitic acid content. The horizontal red
1083 line indicates the significant threshold (10^{-5}). Trait-associated SNPs above the
1084 significant threshold are colored in red.

1085 **Figure S30** GWAS of crude protein content using MLM. **A.** Density distribution of
1086 crude protein content. **B.** Manhattan plots for crude protein content. Negative \log_{10}
1087 P-values from a genome-wide scan are plotted against SNP positions of 20
1088 chromosomes. **C.** Quantile-quantile plot for crude protein content. The horizontal red
1089 line indicates the significant threshold (10^{-5}). Trait-associated SNPs above the
1090 significant threshold are colored in red.

1091 **Figure S31** GWAS of alanine content using MLM. **A.** Density distribution of alanine
1092 content. **B.** Manhattan plots for alanine content. Negative \log_{10} P-values from a
1093 genome-wide scan are plotted against SNP positions of 20 chromosomes. **C.**
1094 Quantile-quantile plot for alanine content. The horizontal red line indicates the
1095 significant threshold (10^{-5}). Trait-associated SNPs above the significant threshold are

1096 colored in red.

1097 **Figure S32** GWAS of arginine content using MLM. **A.** Density distribution of
1098 arginine content. **B.** Manhattan plots for arginine content. Negative \log_{10} P-values
1099 from a genome-wide scan are plotted against SNP positions of 20 chromosomes. **C.**
1100 Quantile-quantile plot for arginine content. The horizontal red line indicates the
1101 significant threshold (10^{-5}). Trait-associated SNPs above the significant threshold are
1102 colored in red.

1103 **Figure S33** GWAS of aspartic acid content using MLM. **A.** Density distribution of
1104 aspartic acid content. **B.** Manhattan plots for aspartic acid content. Negative \log_{10}
1105 P-values from a genome-wide scan are plotted against SNP positions of 20
1106 chromosomes. **C.** Quantile-quantile plot for aspartic acid content. The horizontal red
1107 line indicates the significant threshold (10^{-5}). Trait-associated SNPs above the
1108 significant threshold are colored in red.

1109 **Figure S34** GWAS of glutamate content using MLM. **A.** Density distribution of
1110 glutamate content. **B.** Manhattan plots for glutamate content. Negative \log_{10} P-values
1111 from a genome-wide scan are plotted against SNP positions of 20 chromosomes. **C.**
1112 Quantile-quantile plot for glutamate content. The horizontal red line indicates the
1113 significant threshold (10^{-5}). Trait-associated SNPs above the significant threshold are
1114 colored in red.

1115 **Figure S35** GWAS of glycine content using MLM. **A.** Density distribution of glycine
1116 content. **B.** Manhattan plots for glycine content. Negative \log_{10} P-values from a
1117 genome-wide scan are plotted against SNP positions of 20 chromosomes. **C.**

1118 Quantile-quantile plot for glycine content. The horizontal red line indicates the
1119 significant threshold (10^{-5}). Trait-associated SNPs above the significant threshold are
1120 colored in red.

1121 **Figure S36** GWAS of histidine content using MLM. **A.** Density distribution of
1122 histidine content. **B.** Manhattan plots for histidine content. Negative \log_{10} P-values
1123 from a genome-wide scan are plotted against SNP positions of 20 chromosomes. **C.**
1124 Quantile-quantile plot for histidine content. The horizontal red line indicates the
1125 significant threshold (10^{-5}). Trait-associated SNPs above the significant threshold are
1126 colored in red.

1127 **Figure S37** GWAS of isoleucine content using MLM. **A.** Density distribution of
1128 isoleucine content. **B.** Manhattan plots for isoleucine content. Negative \log_{10} P-values
1129 from a genome-wide scan are plotted against SNP positions of 20 chromosomes. **C.**
1130 Quantile-quantile plot for isoleucine content. The horizontal red line indicates the
1131 significant threshold (10^{-5}). Trait-associated SNPs above the significant threshold are
1132 colored in red.

1133 **Figure S38** GWAS of leucine content using MLM. **A.** Density distribution of leucine
1134 content. **B.** Manhattan plots for leucine content. Negative \log_{10} P-values from a
1135 genome-wide scan are plotted against SNP positions of 20 chromosomes. **C.**
1136 Quantile-quantile plot for leucine content. The horizontal red line indicates the
1137 significant threshold (10^{-5}). Trait-associated SNPs above the significant threshold are
1138 colored in red.

1139 **Figure S39** GWAS of lysine content using MLM. **A.** Density distribution of lysine

1140 content. **B.** Manhattan plots for lysine content. Negative \log_{10} P-values from a
1141 genome-wide scan are plotted against SNP positions of 20 chromosomes. **C.**
1142 Quantile-quantile plot for lysine content. The horizontal red line indicates the
1143 significant threshold (10^{-5}). Trait-associated SNPs above the significant threshold are
1144 colored in red.

1145 **Figure S40** GWAS of methionine content using MLM. **A.** Density distribution of
1146 methionine content. **B.** Manhattan plots for methionine content. Negative \log_{10}
1147 P-values from a genome-wide scan are plotted against SNP positions of 20
1148 chromosomes. **C.** Quantile-quantile plot for methionine content. The horizontal red
1149 line indicates the significant threshold (10^{-5}). Trait-associated SNPs above the
1150 significant threshold are colored in red.

1151 **Figure S41** GWAS of phenylalanine content using MLM. **A.** Density distribution of
1152 phenylalanine content. **B.** Manhattan plots for phenylalanine content. Negative \log_{10}
1153 P-values from a genome-wide scan are plotted against SNP positions of 20
1154 chromosomes. **C.** Quantile-quantile plot for phenylalanine content. The horizontal red
1155 line indicates the significant threshold (10^{-5}). Trait-associated SNPs above the
1156 significant threshold are colored in red.

1157 **Figure S42** GWAS of proline content using MLM. **A.** Density distribution of proline
1158 content. **B.** Manhattan plots for proline content. Negative \log_{10} P-values from a
1159 genome-wide scan are plotted against SNP positions of 20 chromosomes. **C.**
1160 Quantile-quantile plot for proline content. The horizontal red line indicates the
1161 significant threshold (10^{-5}). Trait-associated SNPs above the significant threshold are

1162 colored in red.

1163 **Figure S43** GWAS of serine content using MLM. **A.** Density distribution of serine
1164 content. **B.** Manhattan plots for serine content. Negative \log_{10} P-values from a
1165 genome-wide scan are plotted against SNP positions of 20 chromosomes. **C.**
1166 Quantile-quantile plot for serine content. The horizontal red line indicates the
1167 significant threshold (10^{-5}). Trait-associated SNPs above the significant threshold are
1168 colored in red.

1169 **Figure S44** GWAS of threonine content using MLM. **A.** Density distribution of
1170 threonine content. **B.** Manhattan plots for threonine content. Negative \log_{10} P-values
1171 from a genome-wide scan are plotted against SNP positions of 20 chromosomes. **C.**
1172 Quantile-quantile plot for threonine content. The horizontal red line indicates the
1173 significant threshold (10^{-5}). Trait-associated SNPs above the significant threshold are
1174 colored in red.

1175 **Figure S45** GWAS of tyrosine content using MLM. **A.** Density distribution of
1176 tyrosine content. **B.** Manhattan plots for tyrosine content. Negative \log_{10} P-values
1177 from a genome-wide scan are plotted against SNP positions of 20 chromosomes. **C.**
1178 Quantile-quantile plot for tyrosine content. The horizontal red line indicates the
1179 significant threshold (10^{-5}). Trait-associated SNPs above the significant threshold are
1180 colored in red.

1181 **Figure S46** GWAS of valine content using MLM. **A.** Density distribution of valine
1182 content. **B.** Manhattan plots for valine content. Negative \log_{10} P-values from a
1183 genome-wide scan are plotted against SNP positions of 20 chromosomes. **C.**

1184 Quantile-quantile plot for valine content. The horizontal red line indicates the
1185 significant threshold (10^{-5}). Trait-associated SNPs above the significant threshold are
1186 colored in red.

1187 **Figure S47** GWAS of total amino acids content using MLM. **A.** Density distribution
1188 of total amino acids content. **B.** Manhattan plots for total amino acids content.
1189 Negative \log_{10} P-values from a genome-wide scan are plotted against SNP positions
1190 of 20 chromosomes. **C.** Quantile-quantile plot for total amino acids content. The
1191 horizontal red line indicates the significant threshold (10^{-5}). Trait-associated SNPs
1192 above the significant threshold are colored in red.

1193 **Figure S48** GWAS of hundred grain weight using MLM. **A.** Density distribution of
1194 one hundred seed weight. **B.** Manhattan plots for hundred grain weight. Negative
1195 \log_{10} P-values from a genome-wide scan are plotted against SNP positions of 20
1196 chromosomes. **C.** Quantile-quantile plot for hundred grain weight. The horizontal red
1197 line indicates the significant threshold (10^{-5}). Trait-associated SNPs above the
1198 significant threshold are colored in red.

1199 **Figure S49** GWAS of pod number per plant using MLM. **A.** Density distribution of
1200 pod number per plant. **B.** Manhattan plots for pod number per plant. Negative \log_{10}
1201 P-values from a genome-wide scan are plotted against SNP positions of 20
1202 chromosomes. **C.** Quantile-quantile plot for pod number per plant. The horizontal red
1203 line indicates the significant threshold (10^{-5}). Trait-associated SNPs above the
1204 significant threshold are colored in red.

1205 **Figure S50** GWAS of pod size using MLM. **A.** Density distribution of pod size. **B.**

1206 Manhattan plots for pod size. Negative \log_{10} P-values from a genome-wide scan are
1207 plotted against SNP positions of 20 chromosomes. **C.** Quantile-quantile plot for pod
1208 size. The horizontal red line indicates the significant threshold (10^{-5}). Trait-associated
1209 SNPs above the significant threshold are colored in red.

1210 **Figure S51** GWAS of seed number per plant using MLM. **A.** Density distribution of
1211 seed number per plant. **B.** Manhattan plots for seed number per plant. Negative \log_{10}
1212 P-values from a genome-wide scan are plotted against SNP positions of 20
1213 chromosomes. **C.** Quantile-quantile plot for seed number per plant. The horizontal red
1214 line indicates the significant threshold (10^{-5}). Trait-associated SNPs above the
1215 significant threshold are colored in red.

1216 **Figure S52** GWAS of seed number per pod using MLM. **A.** Density distribution of
1217 seed number per pod. **B.** Manhattan plots for seed number per pod. Negative \log_{10}
1218 P-values from a genome-wide scan are plotted against SNP positions of 20
1219 chromosomes. **C.** Quantile-quantile plot for seed number per pod. The horizontal red
1220 line indicates the significant threshold (10^{-5}). Trait-associated SNPs above the
1221 significant threshold are colored in red.

1222 **Figure S53** GWAS of seed size using MLM. **A.** Density distribution of seed size. **B.**
1223 Manhattan plots for seed size. Negative \log_{10} P-values from a genome-wide scan are
1224 plotted against SNP positions of 20 chromosomes. **C.** Quantile-quantile plot for seed
1225 size. The horizontal red line indicates the significant threshold (10^{-5}). Trait-associated
1226 SNPs above the significant threshold are colored in red.

1227 **Figure S54** GWAS of seed weight per plant using MLM. **A.** Density distribution of

1228 seed weight per plant. **B.** Manhattan plots for seed weight per plant. Negative \log_{10}
1229 P-values from a genome-wide scan are plotted against SNP positions of 20
1230 chromosomes. **C.** Quantile-quantile plot for seed weight per plant. The horizontal red
1231 line indicates the significant threshold (10^{-5}). Trait-associated SNPs above the
1232 significant threshold are colored in red.

1233 **Figure S55** Gene expression validation of different haplotypes/phenotypes for five
1234 candidate genes. **A.** Phenotype distribution (left) and expression level (right) of *GL3*
1235 for different haplotypes. **B.** Phenotype distribution (left) and expression level (right)
1236 of *GSTL3* for different haplotypes. **C.** Phenotype distribution (left) and expression
1237 level (right) of *GSTT1b* for different haplotypes. **D.** Phenotype distribution (left) and
1238 expression level (right) of *CKX3* for different haplotypes. **E.** Phenotype distribution
1239 (left) and expression level (right) of *CYP85A2* for different haplotypes.

1240

1241